Eur. Phys. J. B **46**, 349–354 (2005)
DOI: 10.1140/epjb/e2005-00259-3

THE EUROPEAN PHYSICAL JOURNAL B

Magnetization studies of the nuclear spin ordered phases of solid ^{3}He in silver sinters

E.A. Schuberth[a], M. Kath, L. Tassini, and C. Millan-Chacartegui

Walther Meissner Institute for Low Temperature Research, Bavarian Academy of Science, D-85748 Garching, Germany

Received 6 December 2004 / Received in final form 3 May 2005
Published online 18 August 2005 –

Abstract. Solid ^{3}He, in the bcc lattice between 34 and 100 bar, exhibits two nuclear magnetic ordered phases in the sub-mK temperature range, the so called U2D2 low (magnetic) field phase and the "high field phase" above 0.4 T. To determine the exact spin structure of these phases we started a project of neutron scattering from the ordered solid in collaboration with the Hahn-Meitner Institute, Berlin, and other European and US groups. For this experiment it is crucial to grow a single crystal within the sinter needed for cooling the solid to temperatures of the order of 500 μK (or even twenty times lower in the case of the hcp lattice which is formed above 100 bar) and to keep it there long enough to measure a magnetic neutron reflection. We studied the growth of crystals in Ag sinters of different pore size and with different growth speeds to find an optimal way to obtain single crystalline samples. As a first diagnostic step we performed pulsed NMR measurements in the ordered phases of solid ^{3}He in a sinter of 2700 Å particle size down to temperatures of 450 μK at various molar volumes. We could keep the samples in the ordered state for as long as 140 h. The second method we used was SQUID magnetometry. For the low field phase T_N was indicated by a drop of the intensity, both in the NMR signal and in the dc magnetization, whereas in the high field phase an increase of about 30% was observed below the ordering temperature. For the fabrication of the sinters a packing fraction of 50% and subsequent annealing proved to be very favorable to obtain cold ordered solid. Furthermore, we find that a paramagnetic surface contribution from a few monolayers of ^{3}He exists down to 500 μK in addition to the bulk magnetization.

PACS. 67.80.Gb Thermal properties – 67.80.Jd Magnetic properties and nuclear magnetic resonance – 75.30.Kz Magnetic phase boundaries (including magnetic transitions, metamagnetism, etc.)

1 Introduction

The spin structures of the nuclear magnetically ordered phases of solid ^{3}He, commonly denoted as low field phase (lfp) and high field phase (hfp) above 0.4 T, especially of the latter one, are still not known exactly. While the low field phase in bulk material most probably has the U2D2 structure proposed by Osheroff et al. [1] with further evidence added by Benoit et al. from neutron scattering data [2], the spin structure of the "weak ferromagnetic" high field phase is only inferred from its magnetization. The theoretical description of the magnetic phase diagram is based on multiple spin exchange processes which lead to competing quantum mechanical exchange interactions. Three and four spin exchange is favored in the dense lattice (bcc structure below 10 MPa and hcp structure above) since two particle exchange requires too much deformation of the lattice. Although this theory has been worked out in a very elaborate way by Roger et al. [3], quantitative details of the experimental phase diagram [4] are still not reproduced. To clarify experimentally the spin structures of the two phases in the sinters needed for cooling and adsorbing the heat released from the neutron absorption in ^{3}He, we started neutron scattering experiments in collaboration with the Hahn-Meitner Institute in Berlin and other European and US groups [5], ultimately to reach even the high pressure hcp ordered phase below 20 μK [6]. For more information see the feasibility study by Siemensmeyer et al. [7]. The present status of this collaboration and first results will be published elsewhere. Crucial requirements for neutron scattering from solid ^{3}He are that a single crystal can be formed in the sinter and that the sample remains in the ordered state long enough to perform neutron scattering experiments. Also it has to be considered that possibly in the small pores of a sinter solid ^{3}He orders differently than in the bulk. In 200 Å solid ^{3}He clusters, for instance, Matsunaga et al. found a transition very different from U2D2 [8]. Results of our pulsed NMR measurements on solid ^{3}He in a nominally 700 Å sinter in the low field phase have been reported in parts before [9] and they are completed here. The most remarkable feature was that the intensity of the NMR Larmor line decreased to nearly zero in the U2D2 phase. A line

[a] e-mail: eschuber@ph.tum.de

splitting, although not as distinct as in Osheroff's work [1], indicating a sample with some favorable oriented crystallites could be observed but also with very low intensity. We wanted to check if the low NMR intensity reflects the true magnetization of the ordered solid with an independent method, the dc magnetization measured with a SQUID magnetometer. By varying the sinter fabrication and the crystal growth times we tried to find the optimal way to grow single crystals in sinters.

2 Experiment

The NMR setup can be found in our previous publication [9] and only a short description is given here. The NMR H_1 (and pickup) coil was wound around a cylindrical Ag sinter which was pressed around a central cooling rod, also made of Ag. This arrangement was immersed in a pressure cell body, also filled with Ag sinter with a total volume of 0.8 cm^3. The cell was attached to the nuclear cooling stage and mounted in the center of an 8 T superconducting magnet. Pulsed NMR measurements were performed at frequencies between 200 kHz and 1 MHz where the expected line splitting occurs most favorably.

The dc magnetization was measured with a homemade rf SQUID detection system, see e.g. [10] consisting of an astatic pair of pickup coils with 6 mm inner diameter into which the extension of a pressure cell was mounted. This extension was filled with initially 700 Å silver powder which was pressed and annealed in different ways. The solid ^{3}He inside the pickup coil is cooled through this sinter. The cell body itself was again cooled by a Ag rod coming from the nuclear stage. Our silver is all of 5 N purity and usually annealed at 800 °C. The cell design is shown in Figure 1.

Cooling was provided by a 0.9 mole $PrNi_5$ nuclear demagnetization stage whose temperature and warm-up behavior after demagnetization, see Figure 2, was monitored by pulsed NMR on the ^{63}Cu isotope in a high purity Cu sample screwed to the nuclear stage. Here a measuring field of 45 mT was used, big enough that the two Cu isotope lines are well separated in the spectrum. The pulse interval was 4 h, long enough to ensure full recovery of the Cu nuclear polarization and of the solid equilibrium temperature. From the warming rate below 1 mK and knowing the specific heat capacity of our nuclear stage [11], we calculated the warming under neutron irradiation of the Berlin pressure cell which is attached to a nearly identical nuclear stage. This simulation gave a time interval of the order of 30 min during which the solid ^{3}He sample should stay in the ordered phase, long enough to search for the expected ($\frac{1}{2}$, 0, 0) reflection of the U2D2 phase once the crystal orientation is found at high temperature. The faster warming in Figure 2 after 160 h is due to additional external heating.

2.1 Sinter preparation

In principle the sinter should be as dense as possible to absorb as much heat as possible from the decay products of the neutron capture reaction (proton + triton). So we started with a "Pt black" powder with 100 Å particle size. But solid ^{3}He would not grow in it homogeneously and therefore our sinters were all formed from 700 Å "Japanese powder" under different pressures which of course gives different packing fractions. According to our previous experience, pre-sintering at 120 to 130 °C gives good results for thermal conductance of the sinters and so we used pre-sintered powder only. Further heat treatment was done only for one SQUID measurement, in the other cases especially in the NMR part of this work the sinters were used as pressed initially.

The determination of the specific area of our sinters gave 5.2 m^2/cm^3 for the pre-sintered nominally 700 Å powder and 3.3 m^2/cm^3 for the annealed sinter #3 in the SQUID cell, both with 50% packing fraction. A simple estimate, assuming that for a packing fraction of 50% half of the cell volume is filled with spheres of radius r and that 20% of the surface area is lost due to contact regions, gives about 15 m^2/cm^3 nominal specific area for 700 Å

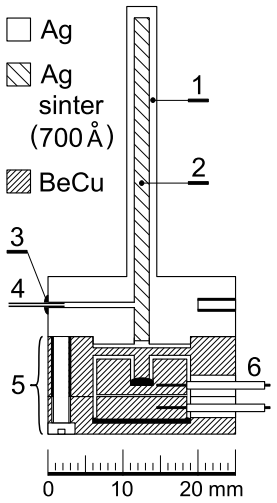

Fig. 1. Drawing of pressure cell (Ag) with extension to fit into SQUID magnetometer and with capacitive Straty-Adams transducer. The extension was filled with different sinters made from initially 700 Å powder.

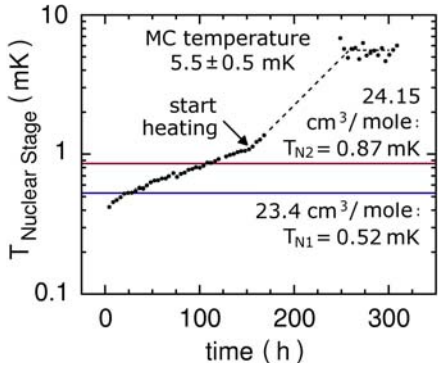

Fig. 2. Temperature of the nuclear stage after demagnetization, determined by pulsed NMR on ^{63}Cu. The residual heat leak is 7 nW, the faster warming after 160 h is due to external heating.

Table 1. Properties of the sinters which were used for the SQUID magnetometry. All powder was "pre-sintered" in vacuum at 130 °C for 30 min before pressing.

Sinter #	1	2	3 (Annealed @ 142 °C)
filling factor	40%	70%	50%
pore size	2700 Å	2700 Å	4200 Å
specific area	4.2 m^2/cm^3	7.2 m^2/cm^3	3.3 m^2/cm^3

particles. 5.2 m^2/cm^3 would be reached with 2700 Å spheres, and 3.3 m^2/cm^3 is provided by 4200 Å ones. So, obviously, in our presinter process we cluster the 700 Å particles to 2700 Å ones. The additional annealing of our third sinter increases this value to 4200 Å. The first sinter with 40% packing fraction had additionally large empty regions so that large parts of the solid did not become cold and ordered. The second sinter with 70% packing fraction was pressed too tight so that solid was not well formed inside and no useful results could be obtained. Finally, the third sinter with 50% packing fraction and annealed finally was most suitable for obtaining cold and well ordered solid. Table 1 lists the properties of our different sinters.

2.2 Crystal growth and thermometry

We performed several runs with the attempt to grow a single crystal in the sinter, all with the blocked capillary method, starting at slightly different pressures around 5.5 MPa at 4.2 K, see Figure 3. The final pressures ranged from just above the melting curve (3.44 MPa, 24.24 cm^3/mole) to 4.158 MPa (23.4 cm^3/mole). Figure 4 shows the observed transition temperatures in our NMR work along with the phase diagram at different molar volumes as given by Fukuyama et al. [12]. They all fit excellently into this diagram, not only in the high field phase, measured by NMR in 0.44 T, but also in the low field region where data points are missing in Fukuyama's work.

The temperature of the solid inside the sinter can be determined only above T_{Neel} by applying a Curie-Weiss law, or modifications of it (see below), to the magnetization measured by NMR (relative to a calibration point around 20 mK where our main carbon resistor is calibrated), or by the SQUID magnetometer. In the latter case the extrapolation to $T \to \infty$ gives $M = 0$, another calibration point. This is much less reliable in the NMR case due to background problems at higher temperatures. Below T_N the temperature of the ordered solid can only be calculated. We applied a three-stage model to calculate the sinter temperature and finally the solid ^{3}He temperature from the known temperature of the nuclear stage. The crucial point here is the knowledge of the Kapitza resistance between sinter and solid which can be independently determined from thermal relaxation measurements at several temperatures above 1 mK which we obtained by stopping the demagnetization and monitoring the cooling of solid ^{3}He towards the nearly constant nuclear stage

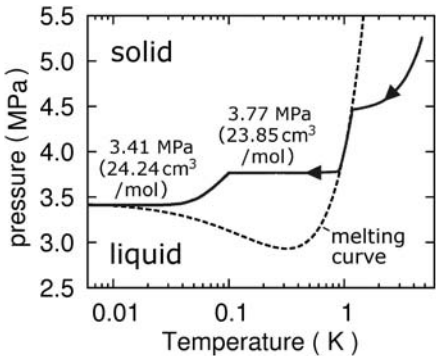

Fig. 3. Crystal growth of solid ^{3}He with the blocked capillary method in the annealed sinter. The pressure drop around 100 mK is due to solid formation in the heat sink closest to the cell.

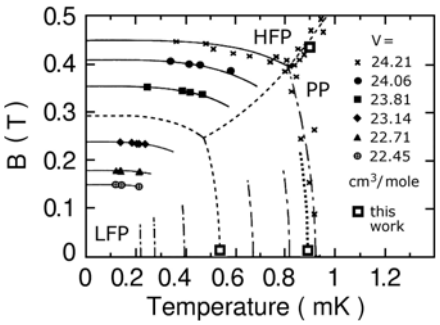

Fig. 4. $B - T$ phase diagram at various molar volumes after Fukuyama et al. [12]. The dash-dotted lines indicate their scaled phase boundaries at low fields. Our proposed transition lines at the molar volumes used in this work (dotted and dashed lines) are shown together with our observed transition temperatures (large open squares).

temperature. The temperature of the solid during the relaxation is taken from its magnetization which in turn is determined under equilibrium conditions by the SQUID magnetometer. Together with the heat capacity which we took from Greywall's work [13] $R_K(T)$ is obtained from a numerical fit to the respective cooling curves giving a T dependence already within one curve. In summary it turned out that the Kapitza resistance for all sinters followed a $T^{-2.5}$ law (with only small variations of the exponent) which we then extrapolated to our lowest temperatures. This calculation gives very plausible warmup curves even around T_N where the heat capacity diverges, see Figure 12, and we believe that the temperatures determined this way are correct to about 10% throughout the measured temperature range, becoming better than 2% around 10 mK. In fact, the perfect match of our transition temperatures to the Fukuyama diagram shows that the error is probably much less than this conservative estimate.

3 Results

The pressures in the solid ^{3}He NMR cell ranged from 3.501 MPa to 4.158 MPa corresponding to molar volumes

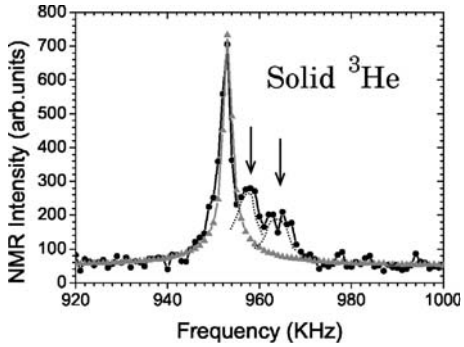

Fig. 5. NMR line splitting in the nuclear ordered state of solid ^{3}He in 29.36 mT. Only two lines at the high frequency side of the Larmor line are found. No other ^{3}He lines occurred in the frequency range from 200 kHz to 3 MHz. The triangles show a scaled line (to match the maximum) from the paramagnetic phase for comparison, the dotted lines are guides to eye to indicate the split line components.

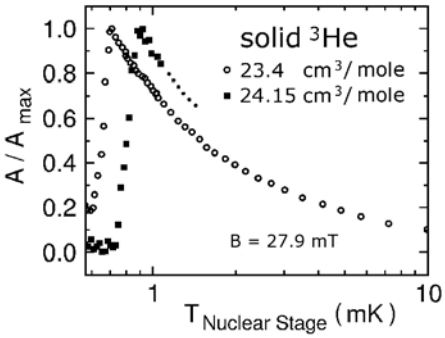

Fig. 6. NMR intensity of the solid ^{3}He Larmor line vs. the cell temperature at 2 different molar volumes: 23.4 cm^3/mole (open circles) and 24.15 cm^3/mole (filled squares). The Neel temperatures, given by the steep rise are 0.52 mK and 0.87 mK respectively, see also Figure 4.

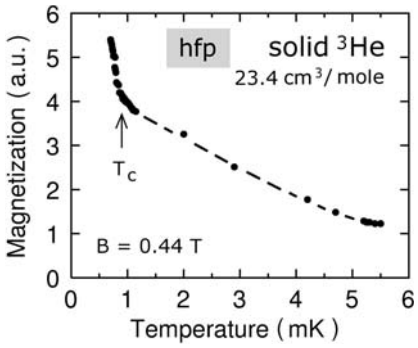

Fig. 7. NMR intensity of solid ^{3}He vs. the cell temperature in the high field phase showing an increase of magnetization below the critical temperature of 0.90(2) mK. The magnetic field was 0.44 T, the molar volume 23.4 cm^3/mole.

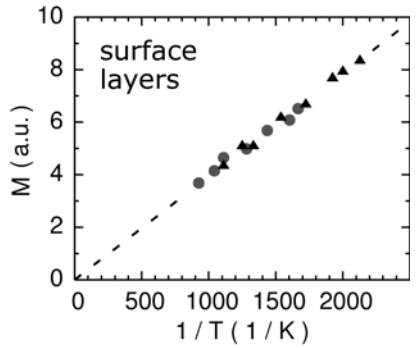

Fig. 8. Contribution to the magnetization background from a few layers of solid around the sinter particles of sinter #3. This surface layer was not removed by cryopumping on the cell at 4.2 K for 12 h. Its proportionality to T^{-1} below T_N shows that this ^{3}He is not in the ordered state.

of 24.15 cm^3/mole and 23.4 cm^3/mole respectively. With fast growth times below 2 h no line splitting could be detected, only a slow growth holding the sample at the melting curve for 6 h resulted in the line splitting shown in Figure 5. But still the intensity of the signal was very low, only 2% of the amplitude just above T_N, see Figure 6. In the high field phase an increase of the NMR intensity in the ordered state is found, see Figure 7, as is expected from previous NMR data [14] and in agreement with multiple spin exchange theories [3] which predict a "canted antiferromagnetic" state with just this magnetization.

SQUID magnetization signals were measured in several sinters and with several solid ^{3}He samples. The final pressures in the SQUID experiments were around 3.44 MPa within a limited range of molar volumes around 24.24 cm^3/mole, the molar volume at the melting curve. In the first two sinters which were not heat treated, the nuclear ordering to the low field phase could hardly be reached, in fact only in one case with a multiple step demagnetization procedure. In this case, the ordering was incomplete and precise data on the magnetization could not be obtained. Only after heat treatment of the third sinter the magnetization of the fully ordered solid could be determined.

The background magnetization of the nominally 700 Å Ag powder proved to be a major problem since its magnetization by far dominated the total signal. Therefore, the background had to be determined very accurately in each run for subtraction. Fortunately, for the empty cell it was essentially flat below 2 mK in 18.5 mT field (our measuring field) and variations below this temperature were only due to the bulk solid signal. With the third sinter, we observed a variation in the ordered state which was proportional to $1/T$ and which thus reflected a Curie law. By loading the surface with about three layers of ^{3}He at 4.2 K, we could see that this signal reoccurred, see Figure 8, and that it must come from a few layers of solid at the surface which do not participate in the U2D2 phase formation. A similar contribution but with no explicitly measured $1/T$ dependence was also noticed by Hata et al. [15]. Usually, the first three layers tend to be ferromagnetic, however, due to frustration effects a nearly paramagnetic T-dependence was found by Bäuerle et al. for ^{3}He on Grafoil down to even lower temperatures than ours [16]. As for the silver sinter magnetic background signal, a Brillouin function fit yielded the best result with a $J = 5/2$ electronic magnetic

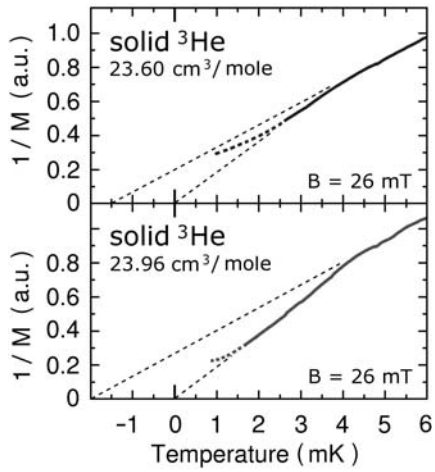

Fig. 9. Inverse magnetization of solid ^{3}He in sinter #1 vs. temperature at two different pressures, molar volumes 23.60 cm^3/mole and 23.96 cm^3/mole. The ordered phase is not reached here, only a small part of the sample is cooled through T_N as indicated by the fat dashed lines. The Weiss temperatures of −1.5 mK (upper part) and −2.0 mK (lower part) reflect the different ordering temperatures for the different molar volumes.

moment in a concentration of about 12 ppm, probably from Fe or Mn impurities.

These contributions were finally subtracted from our raw data. The results for the dc magnetization of solid ^{3}He in 26 mT at two different molar volumes are shown in Figure 9. In this figure several features are remarkable: in the first sinter with a mean packing fraction of 40% the ordered phase could not fully be reached. We assume a pore size distribution ranging from 2700 Å to macroscopic pores in this sinter. For the latter we have indications because when the sinter was drilled out of the cell, hollow portions of it were detected. Then the slight upward bend of the inverse magnetization in the figures obviously stems from solid pores well coupled to the sinter and cooled through T_N. The ordering is however by far not complete (compare Fig. 11) and the solid in the big pores remains above T_N. Above 4 mK both data show a Curie Weiss law with a negative Weiss constant of about −2.0(5) mK, consistent with the observed ordering temperature of 0.9 mK. Both in Figures 9 and 11 the inverse magnetization between 1 mK and 3 mK deviates from the Curie-Weiss law showing a pure Curie behavior. The origin of this is not clear at the moment. Finally, Figures 10 and 11 show the data in the completely ordered state taken in the heat treated sinter #3. Now the sample remained in the ordered phase for 90 h and reached full thermal equilibrium after some 5 h, see Figure 12.

In the NMR case a 47% packed sinter, unannealed, was used which allowed cooling into the ordered state but with long time constants. Probably again, no well ordered (although cold) solid was obtained and thus no distinct splitting of the NMR lines. A broad distribution of crystallites can also lead to a broad distribution of split lines which then disappear in the background.

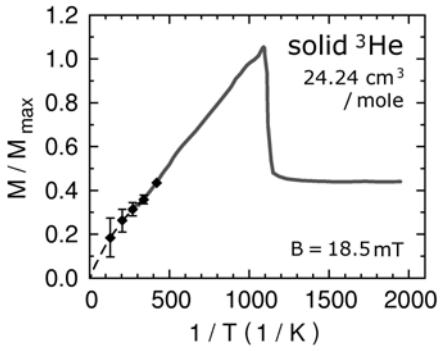

Fig. 10. Normalized magnetization through the nuclear ordering transition of solid ^{3}He vs. inverse temperature in sinter #3. The pressure was just above the melting pressure, molar volume 24.24 cm^3/mole. Here the sample is fully in the ordered state.

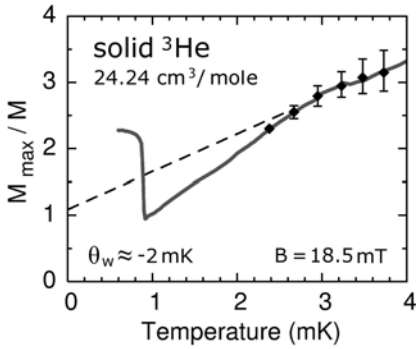

Fig. 11. Data of Figure 10 plotted as inverse magnetization of solid ^{3}He vs. temperature. Both in this figure and in Figure 10 some special points on the continuous curves were selected to show the error bars in the respective T-region.

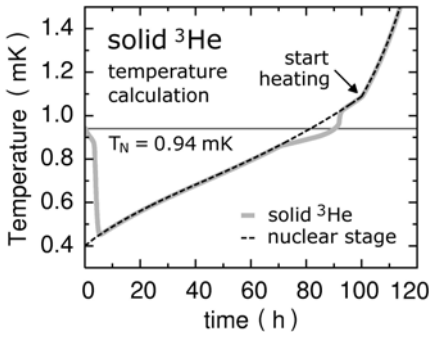

Fig. 12. Calculated solid ^{3}He temperatures for the data of Figures 10 and 11 vs. time after the end of the demagnetization. The initial plateau and the one between 70 and 90 h are due to the latent heat at the first order phase transition from the paramagnetic to low field phase and out of it respectively.

4 Discussion

In both the NMR cell and the SQUID cell, the most successful attempt to grow "good" crystals was to stop the solidification just after reaching the melting curve and then to continue slowly (6 h) to obtain full solidification and additionally 4 h to cool the sample to mK temperatures. The final cell pressure was always somewhat below the value at

which the sample left the melting curve, see Figure 3. The drop around 100 mK is obviously due to recrystallization, or cooling of solid ^{3}He in the heat sink of the filling line since it coincided with the drop in temperature of the final heat exchanger as the phase boundary wandered through it during startup of the dilution refrigerator. This had to be taken into account for the initial pressure in the cells.

Our dc magnetization results show the expected decrease of the solid magnetization in the low field ordered phase, consistent with the U2D2 spin structure. Compared to previous measurements of Hata et al. [15] we observe the same drop down to 40% of the maximum magnetization. The antiferromagnetic exchange interaction tends to order the spins perpendicularly to the external field and the longitudinal magnetization should drop to zero, but the torque of the external field adds a component along its direction. In Roger's original work [3] this parallel component is given by the strengh of the ring exchange contributions in relation to the external torque of the magnetic field on the sublattice magnetization. A drop to 40% of the maximum magnetization is fully consistent with the ring exchange parameters used by Roger et al. to construct their magnetic phase diagram and thus with the U2D2 structure.

The plots of M^{-1} vs. T and of M vs. T^{-1} show a Curie-Weiss law between 10 mK and 3 mK with a small Θ_W of $-2.0(5)$ mK, consistent with the antiferromagnetic U2D2 state. Why there is a pure Curie dependence between 3 mK and 1 mK is not clear at present. There is also the unresolved question why the NMR intensity disappears even when the line splitting indicates a crystalline structure, at least to some extent. We also were not successful in finding the antiferromagnetic resonance around 880 kHz expected for the U2D2 ordered structure [1] or other split off lines, but this can be due to the fact that the sample consisted of a variety of crystallites in this case. Also our line splitting does not comply with the sum rule $\sum_{i=1}^{3} \cos^2 \alpha_i = 1$ required for a single crystallite with 3 domains [1]. As for the growth and cooling ^{3}He crystals for neutron scattering experiments, our present result with the annealed third sinter gives us some encouragement that with even slower growth and cooling rates, a single crystal with a small number of magnetic domains can be grown which is suitable for this purpose. Indeed, the Berlin group was successful in finding sharp structural reflections with similarly grown samples. Cooling into the ordered states has still to be done there.

We gratefully acknowledge financial support from EU, contract HPRN-CT-2000-00166. And we thank Prof. R. Gross of the Walther Meissner Institute for the internal support of the project.

References

1. D.D. Osheroff, M.C. Cross, D.S. Fisher, Phys. Rev. Lett. **44**, 792 (1980)
2. A. Benoit, J. Bossy, J. Schweizer, J. Phys. Lett. **46**, 923 (1985)
3. M. Roger, J.H. Hetherington, J.M. Delrieu, Rev. Mod. Phys. **55**, 1 (1983)
4. J.S. Xia, W. Ni, E.D. Adams, Phys. Rev. Lett. **70**, 1481 (1993)
5. The EU Research and Training Network includes groups from Hahn-Meitner-Institut, Berlin, Royal Holloway University, London, University of Liverpool, both UK, CNRS Grenoble, CEA/DSM, Paris, Saclay, both France, and the University of Florida, USA
6. T. Lang, P.L. Moyland, D.A. Sergatskov, E.D. Adams, Y. Takano, Phys. Rev. Lett. **77**, 322 (1996)
7. K. Siemensmeyer, E.A. Schuberth, E.D. Adams, Y. Takano, K. Guckelsberger, Physica B **284–286**, 363 (2000)
8. N. Matsunaga, V.A. Shvarts, E.D. Adams, J.S. Xia, E.A. Schuberth, Phys. Rev. Lett. **86**, 2365 (2001)
9. E.A. Schuberth, C. Millan-Chacartegui, S. Schöttl, J. Low Temp. Phys. **134**, 637 (2004)
10. E.A. Schuberth, Intern. J. Mod. Phys. B **10**, 357 (1996)
11. M. Kubota, H.R. Folle, Ch. Buchal, R.M. Mueller, F. Pobell, Phys. Rev. Lett. **45**, 1812 (1980)
12. H. Fukuyama, T. Okamoto, T. Fukuda, H. Akimoto, H. Ishimoto, S. Ogawa, Phys. Rev. Lett. **67**, 1274 (1991)
13. D.S. Greywall, P.A. Busch, Phys. Rev. B **36**, 6853 (1987)
14. E.D. Adams, E.A. Schuberth, G. Haas, D. Bakalyar, Phys. Rev. Lett. **44**, 789 (1980)
15. T. Hata, S. Yamasaki, T. Kodama, T. Shigi, J. Low Temp. Phys. **71**, 193 (1988)
16. C. Bäuerle, A.S. Chen, Yu. M. Bunkov, H. Godfrin, M. Roger, J. Low Temp. Phys. **113**, 287 (1998)